Luminescence

Deutsche Ausgabe: DOI: 10.1002/ange.201600241
Internationale Ausgabe: DOI: 10.1002/anie.201600241

Bimetallic Au_2Cu_6 Nanoclusters: Strong Luminescence Induced by the Aggregation of Copper(I) Complexes with Gold(0) Species

Xi Kang, Shuxin Wang, Yongbo Song, Shan Jin, Guodong Sun, Haizhu Yu, and Manzhou Zhu**

Abstract: *The concept of aggregation-induced emission (AIE) has been exploited to render non-luminescent Cu^ISR complexes strongly luminescent. The Cu^ISR complexes underwent controlled aggregation with Au^0. Unlike previous AIE methods, our strategy does not require insoluble solutions or cations. X-ray crystallography validated the structure of this highly fluorescent nanocluster: Six thiolated Cu atoms are aggregated by two Au atoms (Au_2Cu_6 nanoclusters). The quantum yield of this nanocluster is 11.7 %. DFT calculations imply that the fluorescence originates from ligand (aryl groups on the phosphine) to metal (Cu^I) charge transfer (LMCT). Furthermore, the aggregation is affected by the restriction of intramolecular rotation (RIR), and the high rigidity of the outer ligands enhances the fluorescence of the Au_2Cu_6 nanoclusters. This study thus presents a novel strategy for enhancing the luminescence of metal nanoclusters (by the aggregation of active metal complexes with inert metal atoms), and also provides fundamental insights into the controllable synthesis of highly luminescent metal nanoclusters.*

Atomically precise noble-metal nanoclusters (NCs) have attracted extensive research interest,[1–7] and various NCs (such as gold, silver, and bimetallic NCs) have been successfully synthesized in the past decades.[1,8–12] It is generally accepted that the structure of these NCs determines their physical and chemical properties (e.g., the electrochemical,[13] catalytic,[1b,5,14] and optical properties),[9a,15] and is fundamentally important for the related mechanistic studies.[16–18] Among these physical/chemical properties, luminescence represents one of the most fascinating features of these materials.[4,9a,19–21] Luminescent NCs benefit from high biocompatibility, good photostability, and low toxicity, and their use in cell labeling, phototherapy, and biosensing is thus highly promising.[22–24]

To date, several fluorescent noble-metal NCs have been reported.[9a,19–26] Nonetheless, the quantum yield of these NCs remained relatively low compared to those of other fluorescent nanomaterials, such as quantum dots,[27] carbon nanodots,[28] and lanthanide nanoparticles.[29] Therefore, various strategies (e.g., modifying the ligands[30] and/or the metal core)[9a,19] have been developed to enhance the quantum yield of these NCs. The induction of aggregation-induced emission (AIE) has recently become a promising strategy. AIE has previously been reported for solid-state materials (e.g., light-emitting diodes), but the application of this concept to solutions has been challenging for a long time owing to their poor color purity and high instability.[31] In recent studies, solvent- or cation-induced AIE has been successfully applied to rendering metal complexes and NCs fluorescent.[32–35] Nonetheless, the requirement for immiscible solvents or cations limits the application of this strategy.

Considering that AIE mainly induces fluorescence by activating the restriction of intramolecular rotation (RIR),[31] we designed an alternative method to activate RIR. Briefly, the active metal complexes (e.g., Ag or Cu, which are frequently used as fluorescent complexes) could act as the surface ligand, and are controllably aggregated by an inert metal core (such as Au^0). This core–shell structure might hopefully activate the RIR process and boost the AIE of the active metal complexes.

Herein, we report a significant fluorescence enhancement that is induced by the controllable aggregation of non-fluorescent Cu^ISR^1 ($R^1 = C_{10}H_{15}$) with Au^0 atoms, which were generated in situ by the selective reduction of Au^I complexes in the presence of Cu^I complexes. The crystal structure was successfully determined by X-ray crystallography, and the precise composition was identified as $Au_2Cu_6(PPh_2Py)_2(SC_{10}H_{15})_6$ (nanocluster **I**). The movement of the Cu^ISR units was highly restricted by the gold atoms, which led to the high quantum yield of nanocluster **I** (11.7 %). Aside from describing a facile way to synthesize relatively inexpensive, strongly fluorescent NCs, the present study also provides some preliminary mechanistic insights. The RIR-based AIE strategy was confirmed by both DFT calculations and additional control experiments. Furthermore, the DFT calculations revealed that the fluorescence originates from ligand-to-metal charge transfer (LMCT).

The highly fluorescent nanocluster **I** was synthesized in a one-pot process by the selective reduction of phosphine-protected Au^I complexes in the presence of Cu^ISR^1 ($R^1 = C_{10}H_{15}$) complexes. The purity of the product was confirmed by thermogravimetric analysis (TGA), and the weight loss of 66.06 % (see the Supporting Information, Figure S2) is consistent with the calculated loss (66.50 %) of SR^1 and PPh_2Py in nanocluster **I**.

The structure of nanocluster **I** was determined by X-ray crystallography. For clarity, the structure was divided into two parts (the overall structure of **I** is shown in Figure S1). It can be clearly seen that the benzenoid-type outer-loop hexagonal $(CuSR^1)_6$ framework (Figure 1 A) is aggregated by two gold atoms (Figure 1 B). The two gold atoms are further capped by

[*] X. Kang, S. Wang, Y. Song, S. Jin, G. Sun, Prof. H. Yu, Prof. M. Zhu
Department of Chemistry and Center for Atomic Engineering of Advanced Materials, Anhui University
Hefei, Anhui, 230601 (China)
E-mail: yuhaizhu@ahu.edu.cn
zmz@ahu.edu.cn

Supporting information for this article can be found under http://dx.doi.org/10.1002/anie.201600241.

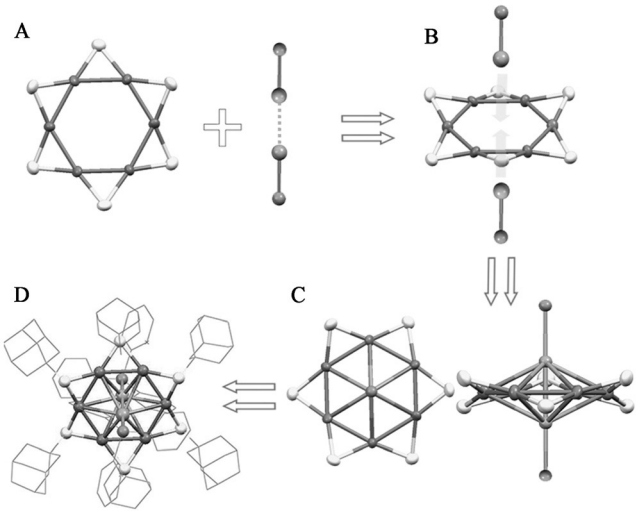

Figure 1. Crystal structure of Au_2Cu_6 nanocluster **I**. A) The outer-loop hexagonal Cu_6S_6 moiety as the benzenoid-like framework of **I**. B) The central Au_2P_2 line across Cu_6S_6. C) Side view and top view of **I**. D) Overall structure of **I**. For clarity, the benzene and pyridine groups on the phosphine ligands and all H atoms are not shown, and the adamantane groups are shown in wireframe.

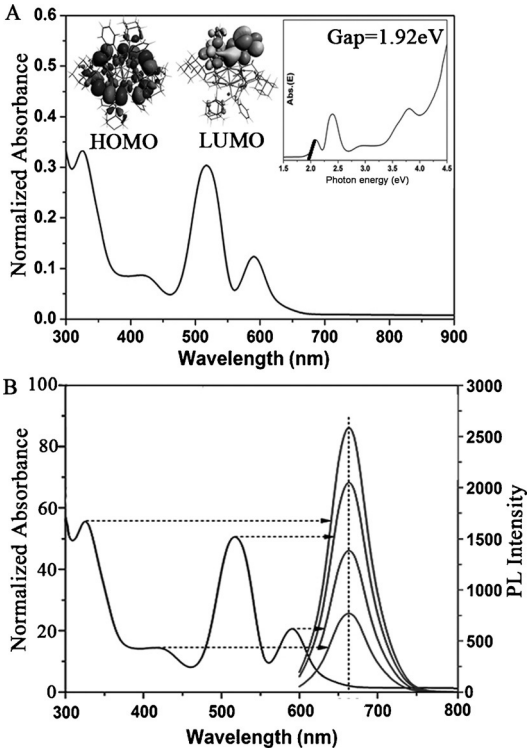

Figure 2. A) Experimental absorption spectrum of nanocluster **I**. Inset: HOMO and LUMO of **I**. B) Photoluminescence properties of **I**. Excitation spectrum (left) and emission spectra (right) at different excitation wavelengths, as indicated by the arrows.

two phosphine ligands. In other words, in Au_2Cu_6 nanocluster **I**, the Au_2@Cu_6 bimetallic core is surface-capped by six thiolates and two phosphine ligands (Figure 1 C, D). The overall nanocluster has a trigonal axis (C_3), three polar axes (C_2), three planes of symmetry (σ_d), and one symmetric center. All of these properties suggest that the point group of nanocluster **I** is D_{3d} (Figure S3).

The UV/Vis spectrum of Au_2Cu_6 nanocluster **I** is shown in Figure 2 A. Aside from the broad multiband optical absorptions centered around 325, 515, and 595 nm, a tail band at 420 nm was observed. Meanwhile, according to the Kohn–Sham (KS) molecular orbital (MO) energy levels in Figure S4, the HOMOs are mainly composed of the S 3p and Cu 3d atomic orbitals. These results indicate that the HOMOs extend to the hexagonal $(CuSR^1)_6$ unit of the overall structure. By contrast, the contributions of the N 2p and C 2p orbitals can be clearly seen in the two lowest, degenerate LUMOs (the N and C atoms all belong to the benzene/pyridine groups of the phosphine ligands), and the upper LUMOs are mainly composed of C 2p atomic orbitals. The KS molecular orbital analysis shows that the Au atoms hardly contribute to the frontier orbitals of Au_2Cu_6 nanocluster **I**.

Interestingly, compound **I** exhibits a strong emission centered at 665 nm with a quantum yield of 11.7 % (Figure 2 B). The PL (photoluminescence) excitation spectrum is almost identical to the absorption spectrum (Figure 2 B). From the UV/Vis spectrum in Figure 2 A, the HOMO–LUMO gap was determined to be 1.92 eV, which is very close to the emission peak (1.87 eV). The extremely low difference in energy (0.05 eV) implies that the fluorescence possibly corresponds to the LUMO–HOMO transition. DFT calculations indicate that the LUMO–HOMO transition predominantly occurs between the ligands (aromatic groups on the phosphine) and the copper centers through weak conjugation of the π-orbitals of the aromatic groups and the Cu d orbitals (see Figure S5 for details). In other words, the emission is due to LMCT, which is similar to the LMCT processes in Ag_{62} and other thiolated metal NCs.[15,17,21b]

Thus far, practical applications of luminescent metal nanoclusters have been limited by the poor understanding of some fundamental aspects, such as the origin of luminescence and size effects. To this end, we intended to clarify the dependence of the fluorescence on the structure of nanocluster **I**. As shown in Figure 3, $AuPR^2Cl$ ($R^2 = Ph_2Py$) was first exposed to the non-emissive $CuSR^1$ complexes, and then the reducing agent $NaBH_4$ was added. The aggregative Au@Cu bimetallic NCs then generate strong luminescence. By contrast, no luminescence was observed in the absence of gold. Meanwhile, the formed products (without Au) showed almost the same properties as the precursor, $CuSR^1$, according to XPS and UV/Vis analysis (Figures S6 and S7), indicating that the Cu^I precursor was not reduced by $NaBH_4$. Furthermore, the XPS spectrum of **I** confirmed the change in the Au valence state (from +1 to 0), while the valence state of Cu remained at +1 (consistent with the XPS of Cu^ISR^1). Therefore, the Au^I species were selectively reduced by $NaBH_4$ (for detailed XPS data, see Table S2). Furthermore, the Au/Cu atomic ratio (1:3) was also confirmed by XPS (Table S1). Compared to the non-luminescent oligomeric Cu^ISR^1 complexes, the Au_2Cu_6 nanocluster **I** shows strong luminescence owing to the Au^0-induced aggregation of the Cu^ISR^1 complexes. This aggregation-based

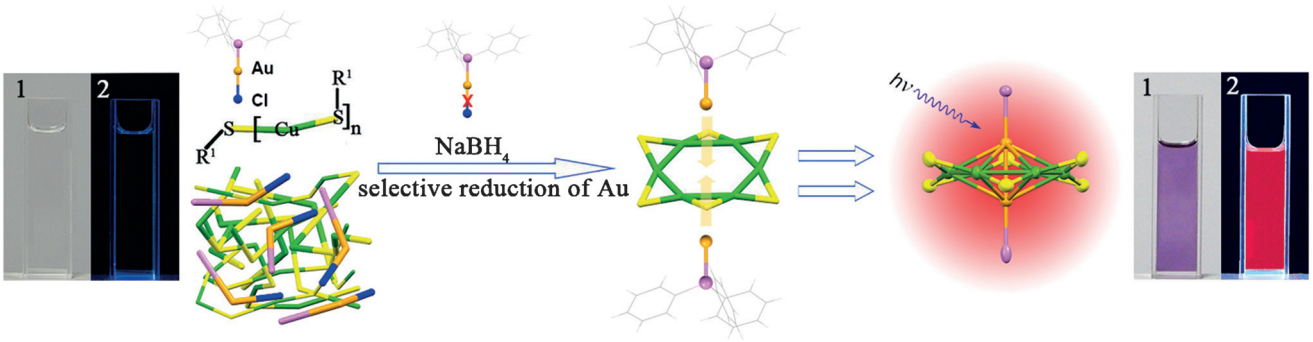

Figure 3. Illustration of the Au^0-induced aggregation of $CuSR^1$. Au^0 was generated by the selective reduction of $AuPR^2Cl$ with $NaBH_4$. Digital photographs of the corresponding complexes or NCs under visible (1) and UV light (2). Au gold, Cl blue, Cu green, P violet, S yellow.

strategy successfully eliminates the necessity for immiscible solvents/cations in previous studies.

As mentioned in the introduction, the AIE is mostly caused by the RIR.[31] Therefore, we expected the fluorescence of the NCs to benefit from the increased rigidity of the capping ligands and the resulting activation of the RIR. To confirm this proposal, we synthesized another Au_2Cu_6 nanocluster (Au_2Cu_6 nanocluster **II**), which was capped by TBM-PPh_2Py ligands (i.e., AdmSH in **I** replaced by *tert*-butyl mercaptan (TBM)). The optical absorption spectrum of **II** strongly resembles that of **I**, implying that the Au_2Cu_6 frameworks are similar in these two NCs (Figure S8). The thermodynamic stability of these two analogous NCs was tested at 30 °C (dissolved in CH_2Cl_2, exposed to air). The optical absorption spectrum of the Au_2Cu_6 nanocluster **I** remained unchanged after twelve hours, whereas that of **II** had already significantly decreased in intensity after one hour, and completely disappeared in approximately three hours (Figure 4). Furthermore, DFT calculations were performed to evaluate the relative stabilities of **I** and **II** by calculating the reaction enthalpy of the ligand-exchange reaction: **I** + 6 TBM → **II** + 6 AdmSH. This reaction was found to be endothermic by 16.10 kcal mol^{-1}, indicating that Au_2Cu_6 species **II** is less stable than **I**. Therefore, both the experimental and theoretical results imply that the structurally less-rigid Au_2Cu_6 nanocluster **II** is less stable.

On the other hand, the luminescence spectra of these two NCs had the same optical density (OD ≈ 0.05), and the maxima in both excitation spectra were located at about 665 nm. As shown in Figure 5, the fluorescence of the more rigid Au_2Cu_6 nanocluster **I** is significantly stronger than that of **II** (with less rigidity). Meanwhile, the Au_2Cu_6 NCs showed

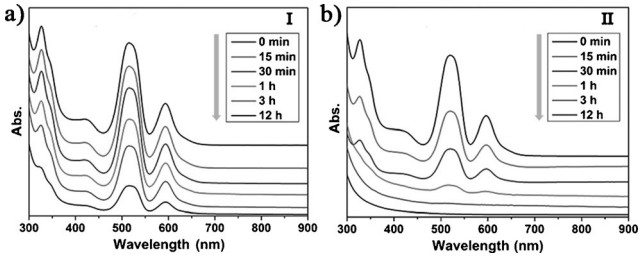

Figure 4. UV/Vis spectra confirming the thermal stability of a) **I** and b) **II** over time.

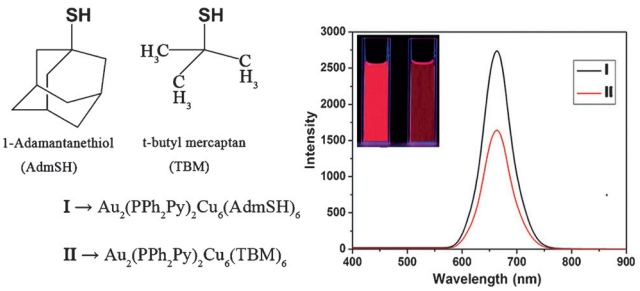

Figure 5. Au_2Cu_6 NCs with different capping ligands and their emission spectra. Digital photographs of solutions of **I** (left) and **II** (right) under UV light.

a significant increase in QY when the capping ligands were strengthened (the QYs of **I** and **II** are 11.7% and 8.0%, respectively). We thus concluded that the enhanced fluorescence of Au_2Cu_6 nanocluster **I** had indeed been achieved by activating the RIR of the outer ligands.

In summary, we have developed a novel strategy to activate aggregation-induced emission, which is based on the aggregation of active metal complexes (Cu^ISR) with neutral gold atoms. The structures of the resulting products (Au_2Cu_6 NCs) were successfully determined by X-ray crystallography, which revealed that six $CuSR^1$ complexes were aggregated by Au^0 atoms. This compound showed strong emission centered at 665 nm with a quantum yield of 11.7%. Furthermore, DFT calculations, additional control experiments, and XPS measurements were used to explore the mechanistic origin of AIE. It was found that the fluorescence is due to ligand-to-metal charge-transfer process. Meanwhile, the rigidity of the ligands positively correlates with the quantum yield, indicating that the AIE is significantly affected by the restriction of intramolecular rotation. Overall, the present study has described the successful synthesis of copper complexes according to the aggregation-induced emission strategy and provided new insights into the strong fluorescence of atomically precise noble-metal nanomaterials.

Experimental Section

Synthesis of $Au_2Cu_6(PPh_2Py)_2(AdmSH)_6$ nanoclusters: CuCl (0.0198 g, 0.2 mmol) was dissolved in CH_3CN (5 mL) and CH_3OH

(5 mL), and AdmSH (0.1346 g, 0.8 mmol) was dissolved in toluene (5 mL). These two solutions were mixed in a 100 mL three-neck round-bottom flask. The overall solution was vigorously stirred (ca. 1200 rpm) by means of a magnetic stirrer for 15 min. Then, [Au(PPh_2Py)Cl] (0.2 g, 0.4 mmol) was dissolved in ice-cold toluene (1 mL), and $NaBH_4$ (80 mg, ca. 5 equiv relative to the gold precursor) was dissolved in 1 mL ice-cold water. Both solutions were added dropwise to the flask at the same time under vigorous stirring. The reaction was allowed to proceed for 60 h under N_2 atmosphere. Afterwards, the reaction mixture was centrifuged to obtain the solids, which were then washed with toluene several times. Then, the final product was dissolved in CH_2Cl_2 and directly crystallized. Nanocluster **I** was crystallized in CH_2Cl_2/hexane at room temperature (ca. 3 days); dark violet crystals were collected and subjected to X-ray diffraction to determine the structure.

The $Au_2Cu_6(PPh_2Py)_2(TBM)_6$ nanoclusters were prepared by the same method as the $Au_2Cu_6(PPh_2Py)_2(AdmSH)_6$ nanoclusters. The amount of *t*BuSH was the same as that of AdmSH.

Synthesis of the $Cu^{I}SR$ complexes (SR = AdmSH): CuCl (0.1 g, 1 mmol) was dissolved in CH_3CN (5 mL). AdmSH (0.18 g, 1.1 mmol) was dissolved in CH_3CN (5 mL) and added to the first solution in a dropwise fashion under vigorous stirring (ca. 1200 rpm) for 15 min. The resulting mixture was then washed with hexane several times. The final product was directly used in the next step.

Acknowledgements

We acknowledge financial support from the NSFC (21372006 and U1532141), the Ministry of Education, the Education Department of Anhui Province, and the 211 Project of Anhui University.

Keywords: aggregation · copper · nanoclusters · gold · luminescence

How to cite: *Angew. Chem. Int. Ed.* **2016**, *55*, 3611 – 3614
Angew. Chem. **2016**, *128*, 3675 – 3678

[1] a) R. Jin, *Nanoscale* **2015**, *7*, 1549 – 1565; b) L. Gao, R. Jin, *Acc. Chem. Res.* **2013**, *46*, 1749 – 1758.
[2] C. P. Joshi, M. S. Bootharaju, O. M. Bakr, *J. Phys. Chem. Lett.* **2015**, *6*, 3023 – 3035.
[3] Y. Tao, M. Li, J. Ren, X. Qu, *Chem. Soc. Rev.* **2015**, *44*, 8636 – 8663.
[4] Z. Luo, K. Zheng, J. Xie, *Chem. Commun.* **2014**, *50*, 5143 – 5155.
[5] S. Yamazoe, K. Koyasu, T. Tsukuda, *Acc. Chem. Res.* **2014**, *47*, 816 – 824.
[6] W. Kurashige, Y. Niihori, S. Sharma, Y. Negishi, *J. Phys. Chem. Lett.* **2014**, *5*, 4134 – 4142.
[7] T. Udayabhaskararao, T. Pradeep, *J. Phys. Chem. Lett.* **2013**, *4*, 1553 – 1564.
[8] A. Das, C. Liu, H. Y. Byun, K. Nobusada, S. Zhao, N. Rosi, R. Jin, *Angew. Chem. Int. Ed.* **2015**, *54*, 3140 – 3144; *Angew. Chem.* **2015**, *127*, 3183 – 3187.
[9] a) S. Wang, X. Meng, A. Das, T. Li, Y. Song, T. Cao, X. Zhu, M. Zhu, R. Jin, *Angew. Chem. Int. Ed.* **2014**, *53*, 2376 – 2380; *Angew. Chem.* **2014**, *126*, 2408 – 2412; b) Y. Song, S. Wang, J. Zhang, X. Kang, S. Chen, P. Li, H. Sheng, M. Zhu, *J. Am. Chem. Soc.* **2014**, *136*, 2963 – 2965; c) S. Yang, J. Chai, Y. Song, X. Kang, H. Sheng, H. Chong, M. Zhu, *J. Am. Chem. Soc.* **2015**, *137*, 10033 – 10035.
[10] H. Yang, Y. Wang, H. Huang, L. Gell, L. Lehtovaara, S. Malola, H. Häkkinen, N. Zheng, *Nat. Commun.* **2013**, *4*, 2422.
[11] a) C. Zeng, Y. Chen, K. Kirschbaum, K. Appavoo, M. Y. Sfeir, R. Jin, *Sci. Adv.* **2015**, *1*, e1500045; b) A. Dass, S. Theivendran, P. R. Nimmala, C. Kumara, V. R. Jupally, A. Fortunelli, L. Sementa, G. Barcaro, X. Zuo, B. C. Noll, *J. Am. Chem. Soc.* **2015**, *137*, 4610 – 4613.
[12] C. P. Joshi, M. S. Bootharaju, M. J. Alhilaly, O. M. Bakr, *J. Am. Chem. Soc.* **2015**, *137*, 11578 – 11581.
[13] S. Park, D. Lee, *Langmuir* **2012**, *28*, 7049 – 7054.
[14] S. Xie, H. Tsunoyama, W. Kurashige, Y. Negishi, T. Tsukuda, *ACS Catal.* **2012**, *2*, 1519 – 1523.
[15] K. Pyo, V. D. Thanthirige, K. Kwak, P. Pandurangan, G. Ramakrishna, D. Lee, *J. Am. Chem. Soc.* **2015**, *137*, 8244 – 8250.
[16] Z. Wu, D. Jiang, A. K. P. Mann, D. R. Mullins, Z. Qiao, L. F. Allard, C. Zeng, R. Jin, S. H. Overbury, *J. Am. Chem. Soc.* **2014**, *136*, 6111 – 6122.
[17] M. Zhou, J. Zhong, S. Wang, Q. Guo, M. Zhu, Y. Pei, A. Xia, *J. Phys. Chem. C* **2015**, *119*, 18790 – 18797.
[18] G. Li, H. Abroshan, Y. Chen, R. Jin, H. J. Kim, *J. Am. Chem. Soc.* **2015**, *137*, 14295 – 14304.
[19] T. Udayabhaskararao, Y. Sun, N. Goswami, S. K. Pal, K. Balasubramanian, T. Pradeep, *Angew. Chem. Int. Ed.* **2012**, *51*, 2155 – 2159; *Angew. Chem.* **2012**, *124*, 2197 – 2201.
[20] Y. Yu, Z. Luo, D. M. Chevrier, D. T. Leong, P. Zhang, D. Jiang, J. Xie, *J. Am. Chem. Soc.* **2014**, *136*, 1246 – 1249.
[21] a) Z. Lei, X. Pei, Z. Jiang, Q. Wang, *Angew. Chem. Int. Ed.* **2014**, *53*, 12771 – 12775; *Angew. Chem.* **2014**, *126*, 12985 – 12989; b) G. Li, Z. Lei, Q. Wang, *J. Am. Chem. Soc.* **2010**, *132*, 17678 – 17679.
[22] C. J. Lin, T. Yang, C. Lee, S. H. Huang, R. A. Sperling, M. Zanella, J. K. Li, J. Shen, H. Wang, H. Yeh, W. J. Parak, W. H. Chang, *ACS Nano* **2009**, *3*, 395 – 401.
[23] J. Yang, N. Xia, X. Wang, X. Liu, A. Xu, Z. Wu, Z. Luo, *Nanoscale* **2015**, *7*, 18464 – 18470.
[24] F. Wen, Y. Dong, L. Feng, S. Wang, S. Zhang, X. Zhang, *Anal. Chem.* **2011**, *83*, 1193 – 1196.
[25] M. S. Bootharaju, C. P. Joshi, M. R. Parida, O. F. Mohammed, O. M. Bakr, *Angew. Chem. Int. Ed.* **2016**, *55*, 922 – 926; *Angew. Chem.* **2016**, *128*, 934 – 938.
[26] L. Shang, S. Dong, G. U. Nienhaus, *Nano Today* **2011**, *6*, 401 – 418.
[27] X. Michalet, F. F. Pinaud, L. A. Bentolila, J. M. Tsay, S. Doose, J. J. Li, G. Sundaresan, A. M. Wu, S. S. Gambhir, S. Weiss, *Science* **2005**, *307*, 538 – 544.
[28] S. N. Baker, G. A. Baker, *Angew. Chem. Int. Ed.* **2010**, *49*, 6726 – 6744; *Angew. Chem.* **2010**, *122*, 6876 – 6896.
[29] F. Wang, X. Liu, *Chem. Soc. Rev.* **2009**, *38*, 976 – 989.
[30] Z. Wu, R. Jin, *Nano Lett.* **2010**, *10*, 2568 – 2573.
[31] Y. Hong, J. W. Y. Lama, B. Z. Tang, *Chem. Soc. Rev.* **2011**, *40*, 5361 – 5388.
[32] Z. Luo, X. Yuan, Y. Yu, Q. Zhang, D. T. Leong, J. Y. Lee, J. Xie, *J. Am. Chem. Soc.* **2012**, *134*, 16662 – 16670.
[33] J. Liang, Z. Chen, J. Yin, G. Yu, S. H. Liu, *Chem. Commun.* **2013**, *49*, 3567 – 3569.
[34] X. Jia, J. Li, E. Wang, *Small* **2013**, *9*, 3873 – 3879.
[35] Z. Wu, J. Liu, Y. Gao, H. Liu, T. Li, H. Zou, Z. Wang, K. Zhang, Y. Wang, H. Zhang, B. Yang, *J. Am. Chem. Soc.* **2015**, *137*, 12906 – 12913.

Received: January 9, 2016
Published online: February 17, 2016

